JOURNAL OF MATERIALS SCIENCE **37** (2002) 3199–3209

Compressive fracture features of syntactic foams-microscopic examination

N. GUPTA*, E. WOLDESENBET
Department of Mechanical Engineering, Louisiana State University, Baton Rouge, LA 70803, USA
E-mail: nikgupt@yahoo.com

KISHORE
Department of Metallurgy, Center for Advanced Studies, Polymer Composite Laboratory, Indian Institute of Science, Bangalore 560012, India

Syntactic foams made by mechanical mixing of polymeric binder and hollow spherical particles are used as core materials in sandwich structured materials. Low density of such materials makes them suitable for weight sensitive applications. The present study correlates various postcompression microscopic observations in syntactic foams to the localized events leading the material to fracture. Depending upon local stress conditions the fracture features of syntactic foam are identified for various modes of fracture such as compressive, shear and tensile. Microscopic observations were also taken at sandwich structures containing syntactic foam as core materials and also at reinforced syntactic foam containing glass fibers. These observations provide conclusive evidences for the fracture features generated under different failure modes. All the microscopic observations were taken using scanning electron microscope in secondary electron mode.
© *2002 Kluwer Academic Publishers*

1. Introduction

Nothing can be more illustrative than microscopy in the investigation of fracture and establishing the causes for it. In case of conventional materials like metals and alloys, relation between the phenomena, which led to fracture and the features of the newly created surface at macro and microscopic level has been studied in great detail over the past several decades. However, for newer materials like syntactic foams, comprehensive microscopic studies cannot be found in the published literature. Syntactic foams are used as core in the sandwich structured materials. Use of syntactic foam as core ensures high rigidity and compressive strength of the sandwich structures compared to other polymeric foams. Other additional advantages gained by the use syntactic foam are low moisture absorption and increased thermal stability. A combination of these properties makes them suitable for structural purpose, especially in aerospace and marine applications. Studies on mechanical properties of syntactic foams [1–3] and their sandwich structures [4–6] can be found in the published literature. However, none of these studies give enough emphasis on microstructural features of the material in pre and post-mechanical test conditions and relate them to the local stress conditions and failure processes.

Polymeric resin acting as binder is mixed mechanically with hollow microspheres, also called microballoons, to make syntactic foam [7–9]. Presence of porosity in closed cell form is responsible for higher compressive strength of syntactic foams compared to the open cell structured polymeric foams. As a consequence of closed porosity, which is in the form of microballoons, elasticity of these materials is less and they are classified in the category of rigid foams. Microspheres incorporated in the binder can be made up of glass, metals or polymers. In the present study syntactic foam slabs were fabricated using glass microspheres along with epoxy resin binder. Fabricated syntactic foam was tested under compressive loading conditions. Specimens having four different aspect ratios, 0.91, 0.67, 0.6 and 0.4 were tested. In case of higher aspect ratios, effect of shear component of the applied compressive stress is prominent, whereas in lower aspect ratio specimens true compression prevails. Testing of specimens of different aspect ratios allow a comparative study of fracture features of syntactic foam in shear and true compression zones of the specimens.

Syntactic foams reinforced with discontinuous glass fibers were also fabricated and tested in this study. Introduction of third component in the structure gives rise to two interfaces namely, resin-microballoons and resin-fibers. In case of syntactic foams having two components, only resin-microballoons interface is present in the system. The difference in interfacial strength due to the presence of two interfaces in a three-component

* Author to whom all correspondence should be addressed.

system helps in establishing a better correlation between fracture features appearing in different parts of a specimen and among different material systems. Microscopic study of syntactic foam in sandwich configurations was also carried out in post-compression test condition. These sandwich configurations having syntactic foam as core material were tested in edgewise as well as flatwise compression mode. In the initial stage of edgewise compressive loading of sandwich material, rigid skins take up major part of the load and transfer only a small part to the foam core. Division of load between two components delays and slows down the crack origination and also the fracture, which effectively causes a magnification effect to the events happening in the material.

Comparison of microscopic fracture features in syntactic foam, reinforced syntactic foam and syntactic foam core sandwich structured composites in various aspect ratios and orientation helped in identifying features of compressive, shear and tensile type of fractures in syntactic foams. Mechanical property data and theoretical analysis of the tests for different materials tested in this study are published separately [10, 11]. The present paper deals exclusively with microscopic analysis of pre and post-mechanical test specimens and establishes the localized mode of fracture.

2. Structure of syntactic foam

Syntactic foams are made by mixing hollow spheres and binder resin by stirring followed by casting in desired shape. In practice it is difficult to avoid entrapment of air in the material system while mixing the constituents, though it can be minimized and maintained at nearly the same level among different specimens by careful processing. The entrapped air is present as open porosity and leads to a three-phase structure in a two component material system. Structure of the fabricated syntactic foam [12] is shown schematically in Fig. 1a. Scanning electron micrograph presented in Fig. 1b shows the surface of a syntactic foam slab. Along with epoxy resin and microballoons, entrapped air pockets (voids) can also be seen in the structure. This micrograph taken from the surface of the material shows only a few microballoons damaged and would serve as a reference while interpreting and comparing the fracture features of various specimens with each other.

3. Materials and fabrication methods

3.1. Syntactic foam

Syntactic foam was fabricated by mechanical mixing of glass microballoons and matrix resin. Very slow hand mixing of the constituents with wooden stirrers was preferred for mixing the materials to minimize the damage to microballoons. Slabs of syntactic foam were cast using unpressurized casting method to avoid any damage to the microballoons during casting. Epoxy resin LY 5052 along with hardener HY 5052, manufactured by Ciba Geigy, was used as matrix material. Microballoons supplied by Grace Electronic Materials, Belgium, having bulk density and true particle densities of 180 kg/m^3 and 254 kg/m^3 respectively were used. Microballoons had average particle diameter of 80 μm. Particle size distribution and compressive strength range of the microballoons provided by the manufacturer are given in Tables I and II, respectively. Cast foam slabs were cured at room temperature overnight and post cured at $130 \pm 3^\circ$C for $2^1/_2$ hr. Dimensions of the cast foam slabs were $150 \times 150 \times 25.4$ mm^3.

TABLE I Particle size distribution of glass microballoons

Particle size range (μm)	Weight fraction
149–175	0.14
125–149	0.10
100–125	0.12
44–100	0.55
<44	0.09

TABLE II Crushing strength of glass microballoons

Stress level (MPa)	%Collapse
3.4	14
6.9	32
13.8	55
20.7	75

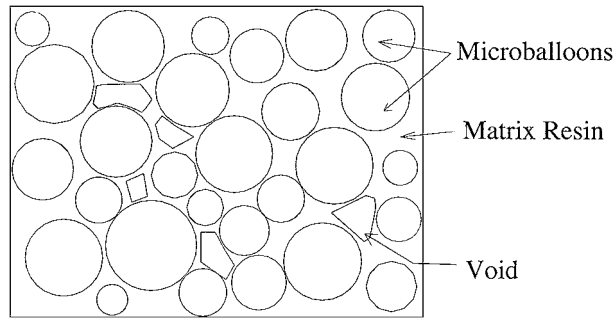

(a)

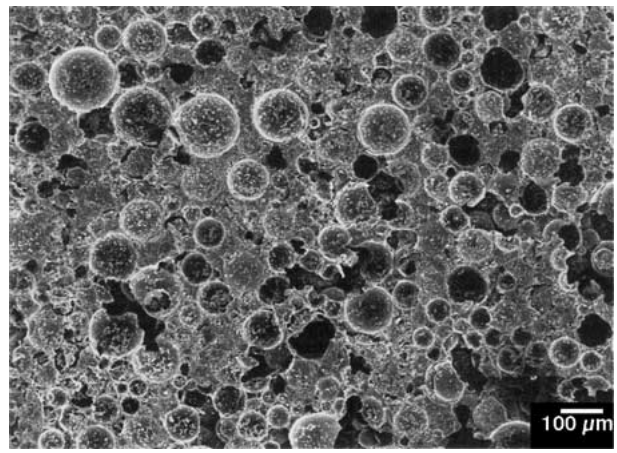

(b)

Figure 1 Three-phase structure of syntactic foam (a) schematic (b) scanning electron micrograph.

3.2. Reinforced syntactic foam

Discontinuous glass fibers were incorporated in the material system along with resin and microballoons to fabricate reinforced syntactic foam slabs. Epoxy compatible E-glass fibers were used for this purpose. Size of the glass fibers was kept below 6 mm to maintain isotropy in the structure. Casting route followed for syntactic foam was used for this material also. Curing

and post curing were also done under same conditions. Good dispersion of fibers and wetting by matrix resin was ensured in the reinforced syntactic foam to obtain homogeneity in the structure.

3.3. Sandwich structures

Some of the syntactic foam slabs were converted into sandwich structures. The cast foam slabs were sectioned to get 6 mm thick slices. On either side of these slices, two layers of 0.2 mm thick epoxy compatible E-glass fabric were attached in 0/90 orientation to form skins. Resin system used for the fabrication of skins was same as that used in fabrication of syntactic foams. Hand lay-up followed by vacuum-bagging was used for the fabrication of sandwich structured materials. Fabricated sandwich materials were cured at room temperature overnight and then post cured at $120 \pm 3^{\circ}$C for $2^{1}/_{2}$ hr.

4. Experimental methods

4.1. Compression testing

Specimens were tested under compressive loading conditions using 100 kN DARTEC-9500 Servo-hydraulic microprocessor controlled mechanical testing machine. Syntactic foam specimens having four different aspect (height/width) ratios 0.4, 0.6, 0.67 and 0.91 were tested under compressive loading conditions. A representative load-displacement curve for syntactic foam is shown in Fig. 2. The typical feature of this curve is the plateau region after yield point. This region is also referred as densification stage where hollow microballoons fracture exposing the hollow space that existed within them, this space is consumed by the material during further compression [11].

Reinforced syntactic foam was tested in two different specimen orientations as indicated schematically in Fig. 3. As the fibers are oriented randomly in these

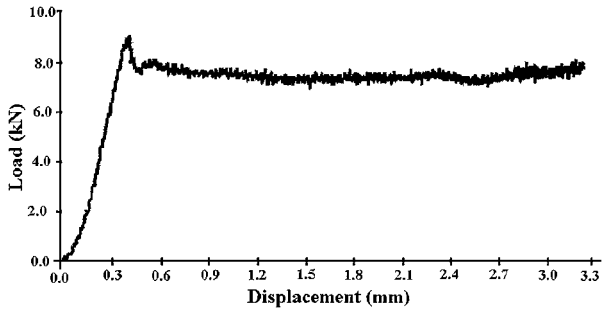

Figure 2 Load–displacement curve for the compression testing of syntactic foam.

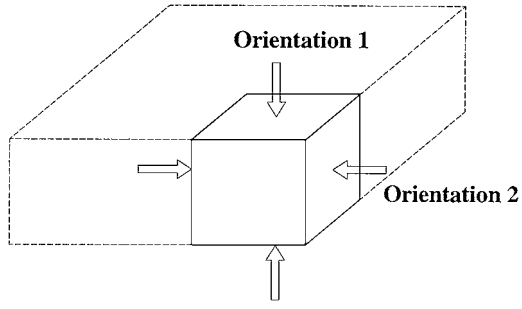

Figure 3 Specimen orientations in compression testing of reinforced syntactic foam.

TABLE III Compressive strength of syntactic foams and their sandwich constructions

Material	Specimen orientation	Average compressive strength (MPa)
Syntactic foam		20.87
Reinforced syntactic foam	Orientation 1	13.67
	Orientation 2	11.58
Glass fabric skin syntactic foam core sandwich	Edgewise	35.25
	Flatwise	21.89

slabs, compression tests in two different orientations were conducted to test the material for isotropy. Fabricated sandwich structures were also tested in two different orientations, namely edgewise and flatwise. In all the tests, constant strain rate of 0.01 s^{-1} was maintained. Compressive strength values for all the materials tested in the study are given in Table III. For syntactic foam the values are average for all the aspect ratios tested in the study.

4.2. Scanning electron microscopy

Syntactic foams and their sandwich structures are polymer based materials and are nonconducting, hence, the specimens were coated with gold before microscopy. Syntactic foams tested in this study are made up of glass hollow spheres, which are brittle. Fracture of syntactic foams gives rise to large amount of broken pieces of microballoons in some of the loading conditions. These loose particles lead to charging during electron microscopic observations of such samples. Hence, the fracture surface of the syntactic foams was subjected to a gentle blow of air before coating the specimens with gold. Scanning electron microscopy of all the specimens was done in secondary electron mode.

5. Syntactic foam specimen failure modes

It is observed during the mechanical testing that the specimen response to the compressive loading depends on the specimen aspect ratio. Sequence of crack origination and subsequent failure in syntactic foam specimens having aspect ratio of 0.4, tested under compressive loading conditions, is shown schematically in Fig. 4. In this case initially shear type cracks originate from the corners of the specimen (marked 1 through 4 in Fig. 4b). However, due to the increased width of the specimen the cracks originating from the opposite corners cannot meet. A horizontal crack (marked as 5 in Fig. 4b) also originates in the specimen due to the true compression in the central region of the specimen. Shear cracks tend to meet the central crack and lead to the formation of wedge shaped fragments at the sidewalls of the specimens. When the specimen having aspect ratios of 0.91 and 0.67 were tested, slight difference was seen in the fracture conditions. The fracture sequence for high aspect ratio specimens is schematically shown in Fig. 5. Shear cracks (marked 1 through 4 in Fig. 5b) appear to originate from the corners of the specimens. With continued compression the cracks forming in the opposite corners of the specimen tend to meet, giving rise to shear type of failure in the specimen. Depending upon the localized conditions either

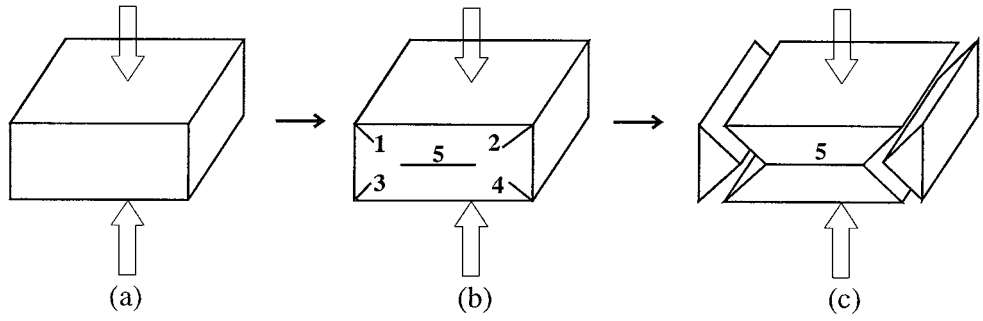

Figure 4 Failure sequence of low aspect ratio (0.4 and 0.6) syntactic foam specimens under compressive loading.

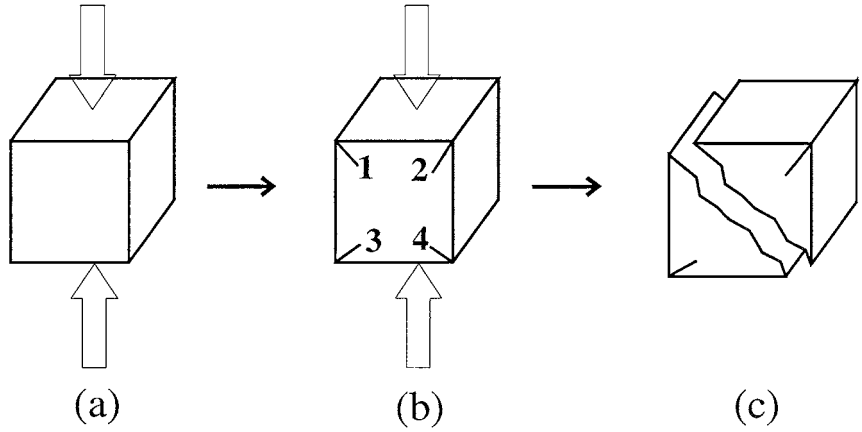

Figure 5 Failure sequence of high aspect ratio (0.91 and 0.67) syntactic foam specimens under compressive loading.

crack 1 can meet crack 4 or crack 2 can meet crack 3. Microscopic observations were taken at the surface of a wedge like fragment separated from the low aspect ratio specimens and at the fracture surface of the high aspect ratio specimens. When top and bottom portions of low aspect ratio specimens were pulled apart, they tend to separate easily along line 5 as shown in Fig. 4c. Observations on these separated surfaces give the actual features of failure under compression, because the compressive load is concentrated in this region. In a two-component material, it is desired to concentrate on damage occurred to both the phases and also to the interface at the fracture surface. In high aspect ratio specimens an interesting observation is that the central zone, which is under compression, lies also on the shear fracture plane. The compression phenomenon will be prevalent in the central region until the shear cracks grow to a substantial length and cause failure of the specimen. Although the final fracture confirms shear type behavior, the features of compression should be preserved in the central region. Locations of the microscopic observations of syntactic foams presented in this study are shown in Fig. 6. Top and bottom uniformly compressed zones and a wedge shaped side chip of low aspect ratio specimens are shown in Fig. 6a and fractured half of the high aspect ratio specimen is shown in Fig. 6b. Large number of micrographs were taken during the microscopy but only a selected few are included in this paper avoiding the redundancy.

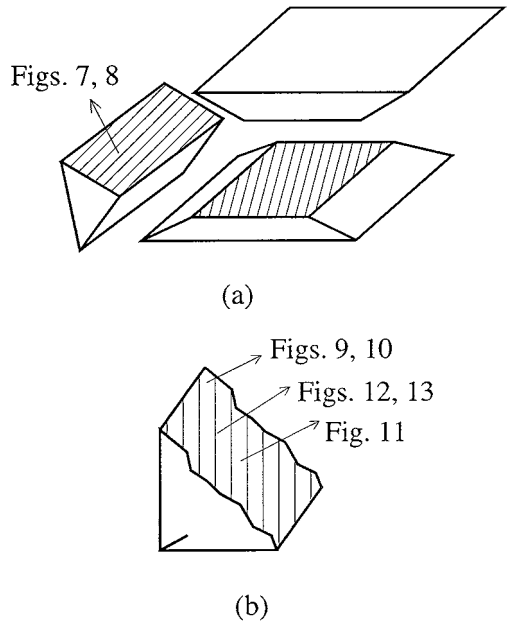

Figure 6 Locations on the (a) low aspect ratio and (b) high aspect ratio syntactic foam specimen surfaces where microscopic observations were taken.

6. Results and discussion

6.1. Microscopic study of syntactic foam

The fractured surface of a fragment separated from the sidewall of a low aspect ratio specimen is shown in Fig. 7. Features to be noted in the micrograph shown in Fig. 7 are the large number of uncrushed microballoons and the small amount of debris. Substantial amount of compression had taken place before the test was stopped, which is evident from the load–displacement curve shown in Fig. 2. Despite such a high degree of compression and glass being brittle material, amount of debris seen in this micrograph is not significant. Hence, the failure mode on this plain is not the compression. High magnification observation of a fractured microballoon embedded in the matrix

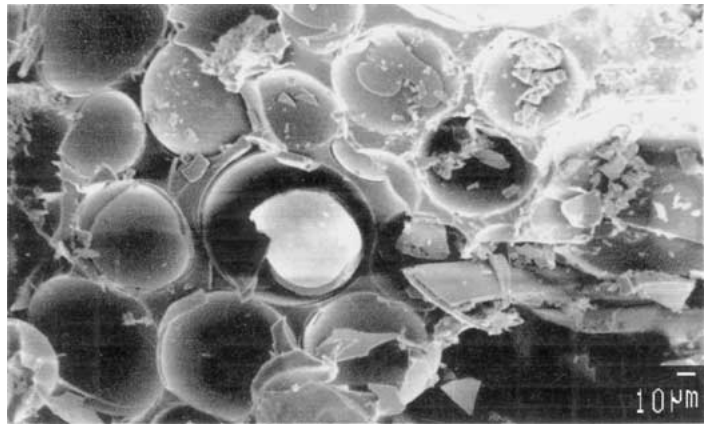

Figure 7 Appearance of fractured surface of sidewall fragment of low aspect ratio specimen.

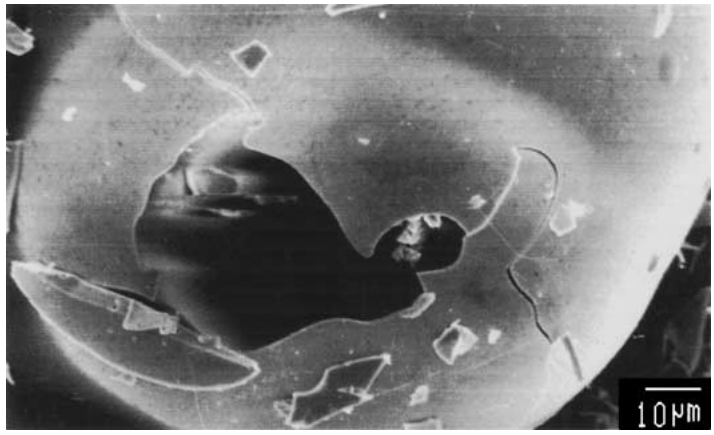

Figure 8 Fracture features of glass microballoon.

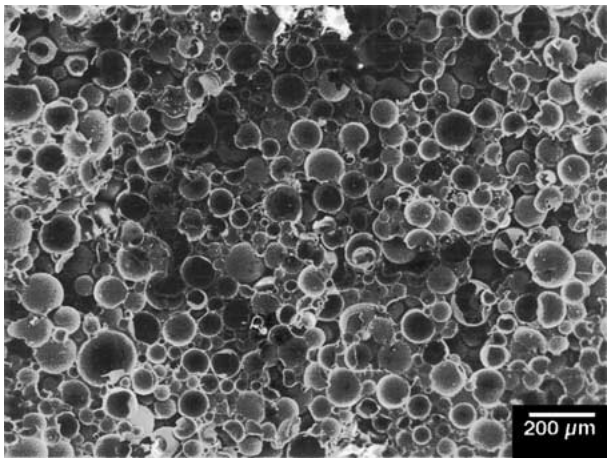

Figure 9 Fractured surface near the corner of the high aspect ratio specimen showing features of shear type of failure.

resin in the same region is shown in Fig. 8. Although the crack has grown to a substantial length, very few fragments are formed from this microballoon. Large number of such microballoons were present in this region. Fig. 9 shows the fractured surface near the corner of a high aspect ratio specimen. Similarity in features can be observed in Figs 7 and 9. Most of the microballoons in both the figures are undamaged. Notable feature is the absence of debris in these micrographs. Careful observation of Fig. 9 reveals the presence of banded structure in this micrograph. The bands appear in steps like fashion in the structure, which form due to the propagation of shear crack at 40–60° angle to the loading axis. Due to this reason, crack frequently changes plane of propagation after small deformation and fracture of a few layers of microballoons in the specimen and produces steps. One such step can be seen near the top left corner in this micrograph. The area shown in Fig. 7, when seen at low magnification to cover more area under the observation, also had the same type of structure. This series of events is unique to the shear type failure and is not possible in compression region where there is no propagation of crack and materials compress uniformly. Observation of the matrix resin at high magnification reveals presence of plastic deformation marks that are also in the form of steps as shown in Fig. 10. This type of marks cannot be generated if the matrix fractures under compression, but are possible in shear type of failure only.

The central part of the same specimen shown in Fig. 11 has considerable difference in appearance of microscopic features. In this region large amount of debris can be seen and undamaged microballoons are absent. As per the earlier discussion, it is expected that this part of the specimen has undergone considerable compression before failure resulting in complete crushing of microballoons. Exactly the same features were observed on the surface of low aspect ratio specimens separated along crack 5 (Fig. 4b) leading to the conclusion that the same deformation and failure phenomena prevailed there also. The region between compression zone and shear zone shows a mixture of these features.

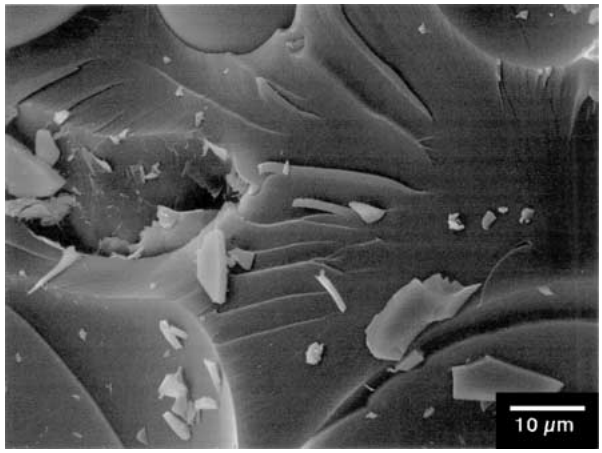

Figure 10 Plastic deformation and fracture pattern in epoxy resin matrix in a region covered in Fig. 9.

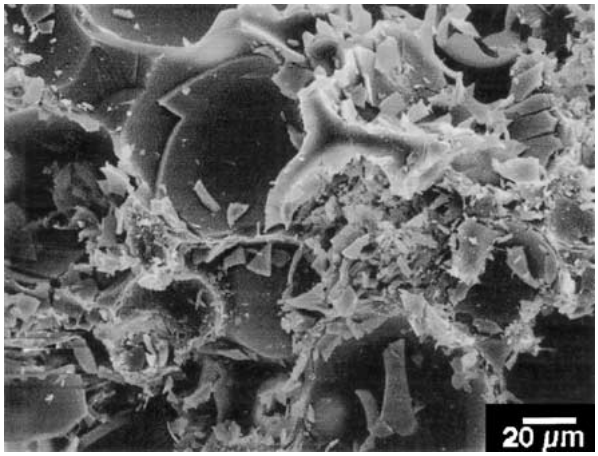

Figure 11 Fractured surface at the center of the high aspect ratio specimen showing features of failure under compression.

Fig. 12 shows a few uncrushed microballoons among the broken ones. High magnification micrograph of the same region (Fig. 13) shows the presence of interfacial separation, which can be attributed to shear forces acting at this point.

6.2. Microscopic study of sandwich configuration

Syntactic foam core is the major load bearing component in the compression testing of syntactic foam core sandwich configuration in flatwise compression mode. Hence, the failure sequence of the material and macroscopic observations are similar to that for the syntactic foam material and are shown schematically in Fig. 14. Cracks marked from 1 through 4 in Fig. 14b are the shear cracks originated in the core and 5 is the crack due to compression of the core. Failure mode in such materials is the failure of syntactic foam core. Hence, the microscopic observations taken for sandwich configurations in flatwise compression failure mode are quite similar to those for syntactic foam material.

Considerable difference is observed in the edgewise compression of sandwich structures using syntactic foams as the core material. The difference in the specimen behavior appears because the load is primarily taken by the rigid skins. Major part of the load is transferred to the core after significant compression of skins or after their fracture. Fig. 15 schematically shows the crack initiation and growth sequence in edgewise compression of sandwich configuration. Fracture features for the plane lying along crack paths 2 and 3 in Fig. 15b generate due to compression and should be similar to that for true compression of syntactic foam. Formation of crack path 1, which is in the direction of the applied compressive stress is possible only under secondary tensile stresses. This crack is expected to show different set of microscopic features due to fracture in different local stress mode, which is a secondary tensile stress.

Surfaces originated along crack 1 shown in Fig. 15 were observed to look for the features of tensile fracture. The surface features such as large number of uncrushed microballoons and very small amount of fragments can be observed in Fig. 16. In this figure steps do not exist on the fracture surface in the form of regular bands or any regular arrangement. Fig. 17 shows magnified view of a small region that was covered in Fig. 16. Contrary to the observations made in shear type of failure shown in Fig. 10, no plastic deformation or fracture pattern was seen in epoxy resin matrix as a general feature for tensile type of failure. On the surface of cracks 2 and 3 illustrated in Fig. 15, the microscopic structure shows typical compressive failure feature, which is the presence of large amount of debris of crushed microballoons (Fig. 18). Undamaged microballoons cannot be seen anywhere in these micrographs.

From the observations in the different modes of failure, it is clear that failure under compression gives rise

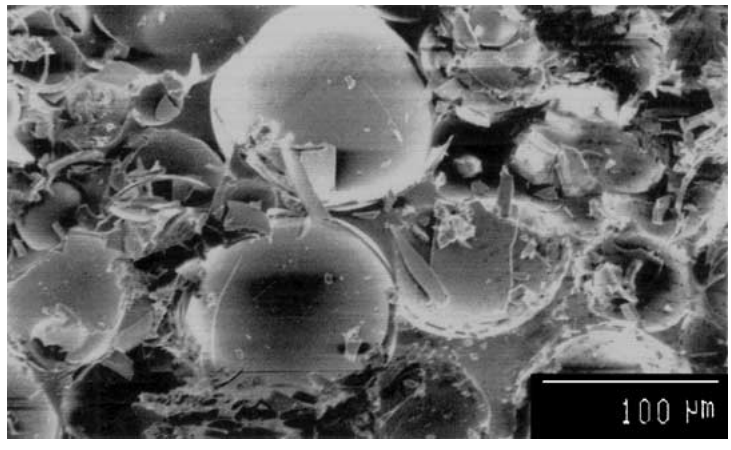

Figure 12 Appearance of fractured surface of high aspect ratio specimen in a region between that in Figs 9 and 11.

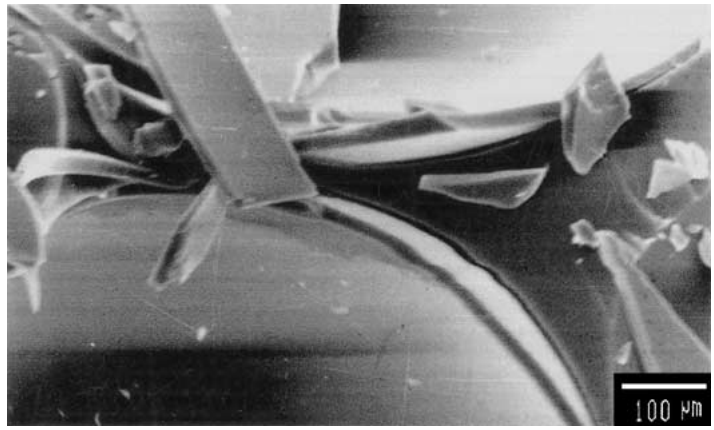

Figure 13 Interfacial separation between microballoon and resin matrix.

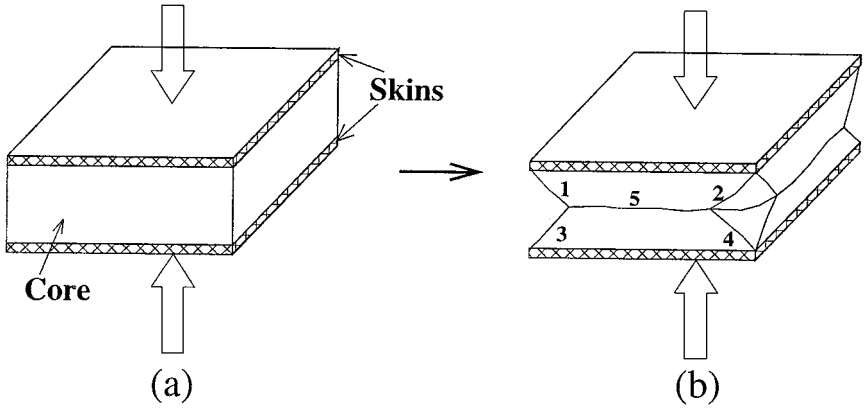

Figure 14 Flatwise compression of syntactic foam core sandwich material.

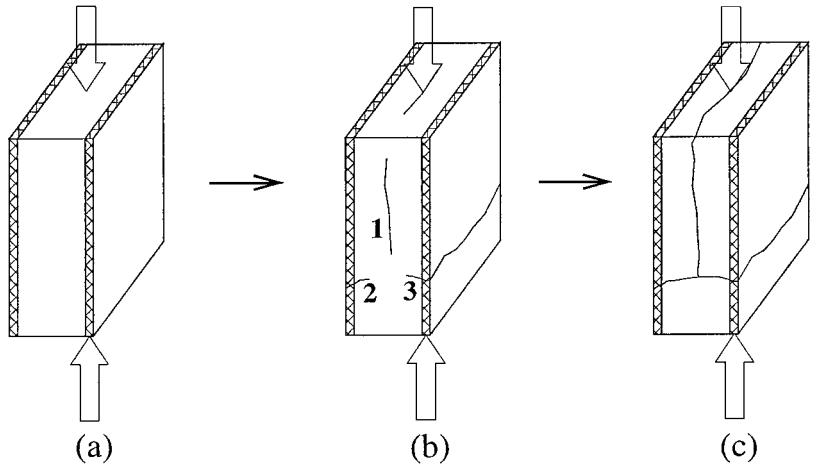

Figure 15 Edgewise compression of syntactic foam core sandwich material.

to large amount of debris in the structure due to brittleness of glass microballoons. Tensile and shear type of failures can be differentiated from compressive failure by the features such as the presence of large amount of undamaged microballoons and absence of debris. To differentiate between tensile and shear type of failure modes, appearance or absence of banded structure must be looked into.

6.3. Microscopic study of reinforced syntactic foam

Use of third component in the structure of syntactic foam is helpful in further strengthening the observations of fracture features in various failure modes. Discontinuous glass fibers were incorporated in the syntactic foams for this purpose. Difference in the interfacial strength between fiber-matrix and matrix-microballoons is helpful in isolating the effect of each component in the process of deformation and fracture by comparing the fracture features of unreinforced and reinforced syntactic foam. These observations can give additional support to the observations made earlier. Low aspect ratio glass fibers were incorporated in well-dispersed form in the syntactic foam. Testing of reinforced syntactic foam in two different orientations (schematically shown in Fig. 3) showed two different types of responses of the specimen to the applied compressive loading conditions. As shown in Fig. 19,

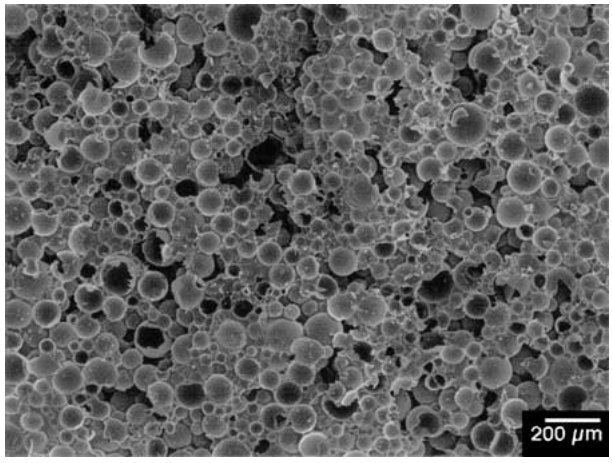

Figure 16 Appearance of surface generated due to the secondary tensile stresses.

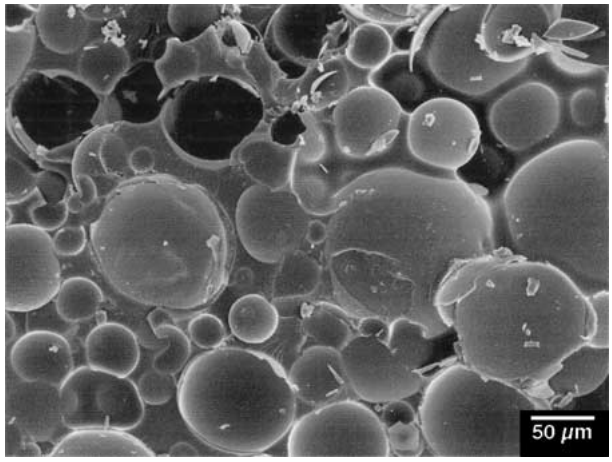

Figure 17 High magnification observation of a region covered in Fig. 16.

specimens in orientation 1 developed a crack and subsequently fractured in the direction of loading. The crack was originated in the early stages of compression and despite separation of specimen into pieces, it kept on resisting the applied load. However, in orientation 2 specimens responded in a manner exactly similar to that for unreinforced syntactic foam, giving rise to wedge shaped fragments from the side walls of the specimens and uniform compression in the central region as shown schematically in Fig. 4. Photograph of a sample tested in orientation 2 is shown in Fig. 20.

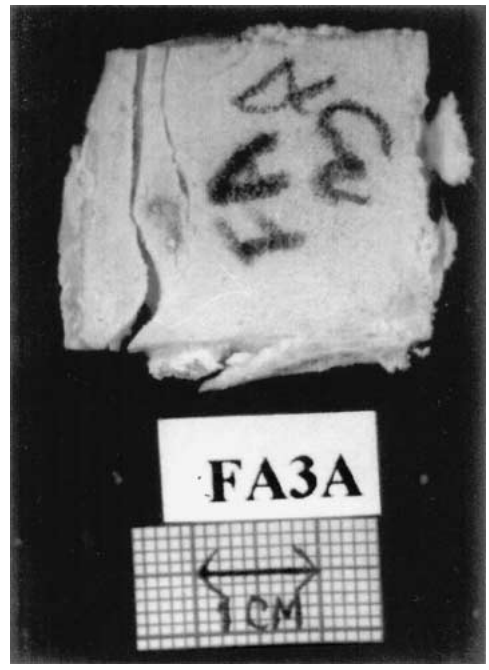

Figure 19 Fracture of reinforced syntactic foam specimen tested under compression in orientation 1.

Microscopic studies of specimen tested in orientation 1 were carried out on the surface generated due to the vertical crack propagation. In the micrographs shown in Fig. 21 large amount of undamaged microballoons were seen along with some damaged ones. Presence of damaged microballoons along with debris can be attributed to the compression of the specimen. However, the vertical crack formation is possible only when fibers are the major load carrier and they tend to buckle considerably before fracture. Hence, the fracture takes place under the secondary tensile force leading to vertical splitting of the specimen. As evident from Fig. 22 interfacial strength between fiber-matrix seems to be better compared to that of microballoon-matrix. Fracture or separation of microballoons from the close vicinity of fibers leaves a hemispherical mark in resin on the surface of fiber. Some hemispherical marks and pieces of broken microballoons adhering to some such marks can be seen in Fig. 22. If tensile forces are absent and only compressive conditions exist, it is expected that these resin marks would be accompanied with large

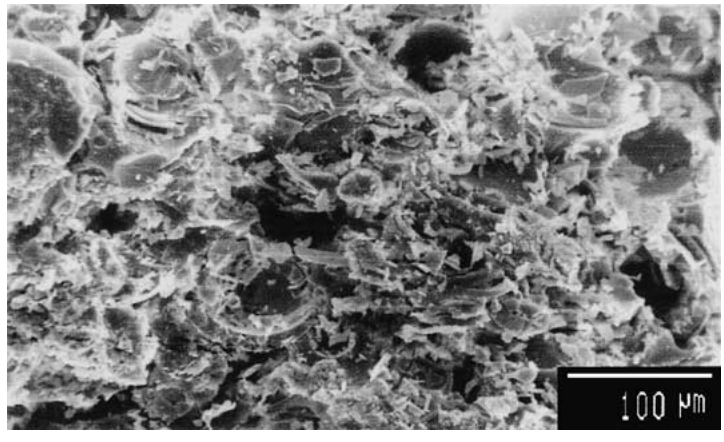

Figure 18 Compressive failure features in syntactic foam core of the sandwich material.

Figure 20 Fracture of reinforced syntactic foam specimen tested under compression in orientation 2.

amount of debris. However, the presence of undamaged microballoons should not be attributed to the presence or absence of any phenomenon. This is due to the fact that the splitting of the specimens occurred in the early stages of compression and the loading was stopped. In later stages of compression the microballoons that are now seen undamaged may also fracture under the applied load, but absence of debris at any stage of compression is the matter of concern.

The central uniformly compressed zone of specimens tested in orientation 2 was microscopically viewed after careful separation. As seen in Fig. 23, fibers are surrounded by small pieces of broken microballoons. Even on close observation (Fig. 24), hemispherical marks on fibers are not seen. Perhaps these marks also fractured during compression as the material has undergone considerable compression. In other parts of the specimen, no undamaged microballoons were found. However, only one totally undamaged microballoon was observed among the debris as shown in Fig. 25 and was looked into with great interest. Closer observations at higher magnifications (Figs 26 and 27) revealed that it was not bonded with any of the adjoining components. Perhaps this microballoon was detached from its site in the early stages of compression leaving a resin mark behind and landed in this crack, which protected it from getting crushed. Comparison of fracture features indicates a preferential orientation of fibers in reinforced syntactic foam specimens. Fibers although discontinuous, are more oriented parallel to the direction of loading when tested in specimen orientation 1 and hence, perpendicular to orientation 2. This changes the loading conditions locally in the specimen and eventually the specimen behavior and reflects into the post compression microstructure.

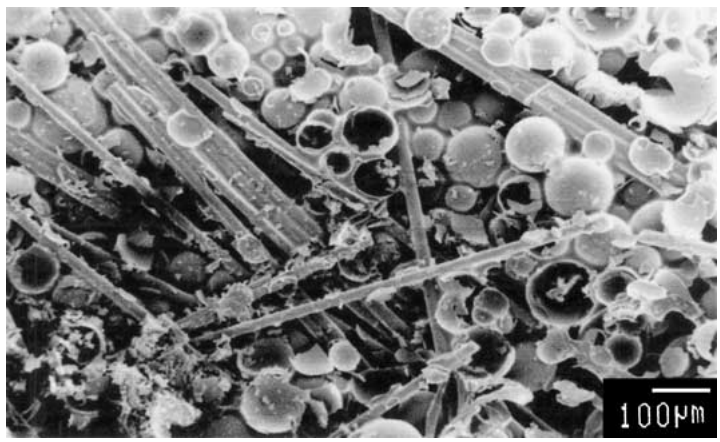

Figure 21 Undamaged microballoons in reinforced syntactic foam specimen tested in orientation 1.

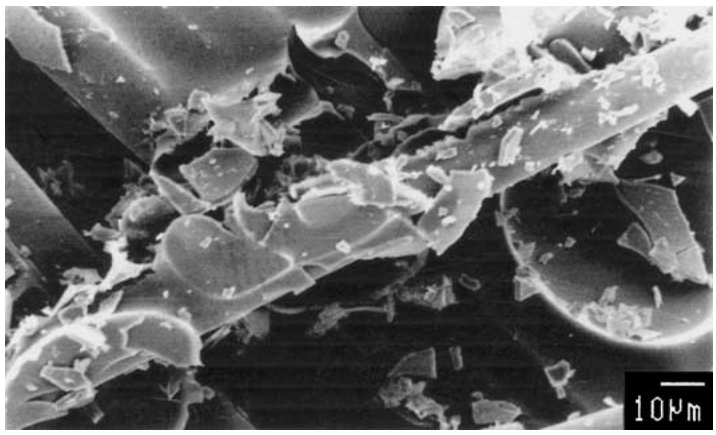

Figure 22 Resin marks on fibers left after fracture of microballoons.

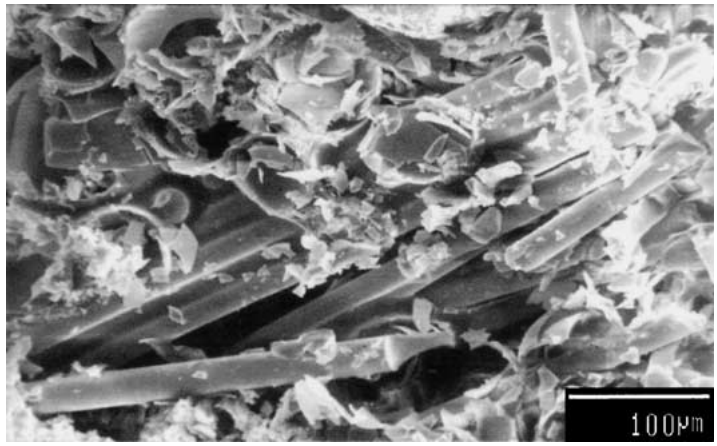

Figure 23 Broken fibers surrounded by fractured microballoons in the reinforced syntactic foam specimen tested in orientation 2.

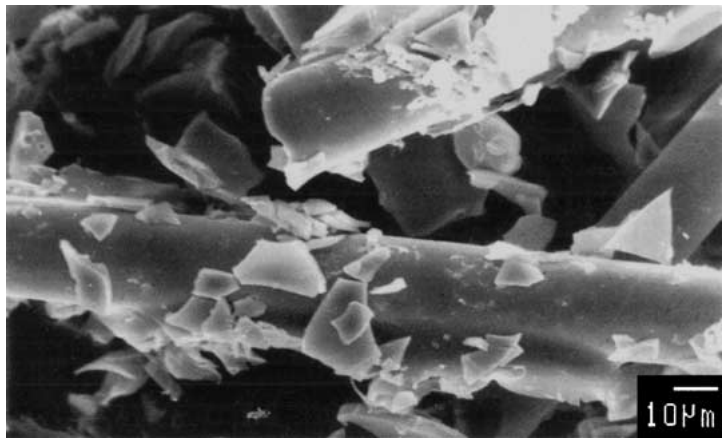

Figure 24 Higher magnification image does not show resin marks left after fracture of microballoons.

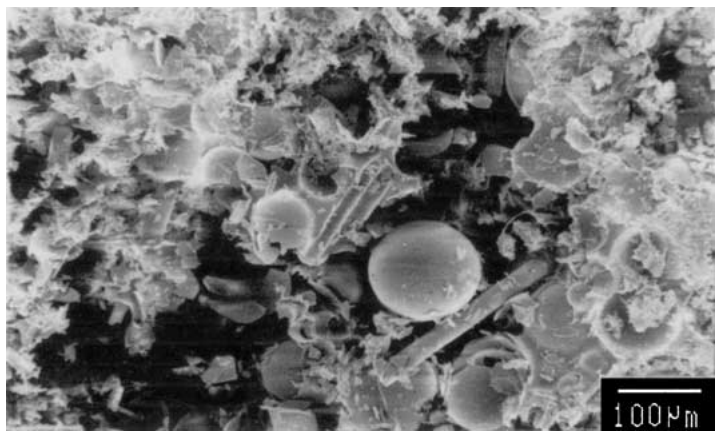

Figure 25 General features of fractured surface of reinforced syntactic foam. Appearance of one undamaged microballoon is unexpected.

Figure 26 Higher magnification micrograph of Fig. 25 for closer observation.

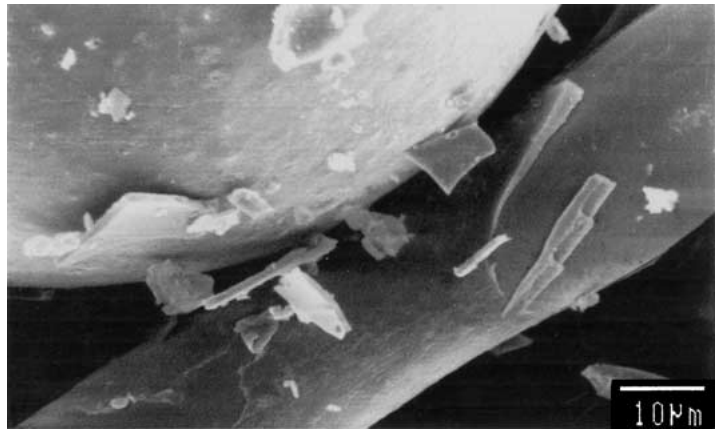

Figure 27 Higher magnification micrograph of Fig. 26 showing no bonding between fiber and microballoon.

7. Conclusions

Comparison of post-compression microstructure of syntactic foam in various parts of the specimens revealed considerable differences, which indicated variations in local stress conditions. Conclusions about the fracture features of syntactic foams in various localized fracture modes were drawn by microscopic observations of the fracture surfaces of syntactic foam tested in four aspect ratios, reinforced syntactic foam tested in two orientations and syntactic foam core sandwich materials in two orientations. As a general feature it could be established that the presence of substantial amount of broken pieces of microballoons on the fracture surface confirms failure under compression mode whereas, absence of debris indicate failure under tensile or shear type of loading conditions. These features are representative of stress conditions prevailed locally. Further, in an attempt to differentiate between features of shear and tensile fracture modes, it is identified that due to frequent change in plane of crack propagation in a specific direction, banded structure appears only in shear type of failure. These bands exist in step like fashion. In tensile failure there is no specific pattern in the appearance of undamaged microballoons, but all over the structure, undamaged microballoons are seen with very few broken fragments. Microscopy of reinforced syntactic foam revealed preferred orientation of fibers, which explained the vertical splitting of specimens in one orientation but not in the other. Macroscopic response of specimen was correlated with the microscopic observations of specimen failure pattern and was found in good agreement.

Acknowledgments

Authors thank Mr. C. S. Karthikeyan, Mr. Jagdish Kumar and Dr. Xiaogang Xie for their help during various stages of processing, testing and microscopy of the materials.

References

1. E. RIZZI, E. PAPA and A. CORIGLIANO, *Intl. J. Solids and Structures* **37** (2000) 5773.
2. K. ASHIDA, in "Handbook of Plastic Foams," edited by A. H. Landrock (Noyes Publishers, New Jersey, 1995) p. 147.
3. F. A. SHUTOV, in "Handbook of Polymeric Foams and Foam Technology," edited by D. Klempner and K. C. Frisch (Hanser Publishers, New York, 1991) p. 355.
4. A. CORIGLIANO, E. RIZZI and E. PAPA, *Compo. Sci. Tech.* **60** (2000) 2169.
5. O. ISHAI, C. HIEL and M. LUFT, *Composites* **26**(1) (1995) 47.
6. C. HIEL, D. DITTMAN and O. ISHAI, *ibid.* **24**(5) (1993) 447.
7. R. A. MALLOY and J. A. HUDSON, in "Foamed Composites in International Encyclopedia of Composites," Vol. 2 (VCH Publishers, New York, 1990) p. 257.
8. N. GUPTA, C. S. KARTHIKEYAN, S. SANKARAN and KISHORE, *Mater. Charat.* **43** (1999) 271.
9. S. SANKARAN, PhD thesis, Department of Chemical Engineering, Indian Institute of Science, Bangalore, India, 1997.
10. N. GUPTA, S. SANKARAN and KISHORE, *J. Reinf. Plast. and Comp.* **18**(4) (1999) 1347.
11. N. GUPTA, KISHORE, E. WOLDESENBET and S. SANKARAN, *J. Mater. Sci.* **36**(18) (2001) 4485.
12. F. A. SHUTOV, *Adv. Ploy. Sci.* **73** (1985) 63.

Received 23 July 2001
and accepted 11 April 2002